Available online at www.sciencedirect.com
ScienceDirect
Scripta Materialia 63 (2010) 565–568
Scripta MATERIALIA
www.elsevier.com/locate/scriptamat

Densification behavior of a fine-grained $MgAl_2O_4$ spinel during spark plasma sintering (SPS)

Koji Morita,* Byung-Nam Kim, Hidehiro Yoshida and Keijiro Hiraga

National Institute for Materials Science, Nano-Ceramics Center, 1-2-1 Sengen, Tsukuba, Ibaraki 305-0047, Japan

Received 12 May 2010; accepted 5 June 2010
Available online 10 June 2010

The densification rate of a spinel during spark plasma sintering can be characterized by the decreasing stress exponent from $\geqslant 4$ to ≈ 1 as the density increases. Transmission electron microscopy observations showed that stacking faults introduced by partial dislocations are observed in a low-density region, but limited in a high-density region. These results suggest that the dominant densification mechanism changes with density, from plastic flow caused by a partial dislocation motion to diffusion creep as the density increases.

Keywords: Powder consolidation; Spark plasma sintering; Ceramics; Deformation structure

The spark plasma sintering (SPS) technique has been applied to the densification of various types of materials [1,2] instead of hot-pressing (HP) or hot-isostatic pressing (HIP) techniques. This is because, compared to the HP or HIP techniques, the SPS technique can produce dense materials within a short time at low temperatures. Using the SPS technique, for example, a magnesium aluminate spinel ($MgAl_2O_4$) having a good transparency can be attained after only a 20 min soak at a low temperature of 1300 °C without any sintering aids [3,4].

In order to clarify the enhanced densification during the SPS process, it is necessary to understand the rate-controlling mechanisms. For SPS processing, however, the rate-controlling mechanism is complicated [5] and hence remains unsolved. The present study was performed to discuss the densification mechanisms of a fine-grained spinel during SPS processing. In this study, the rate-controlling mechanisms were examined by combining the analysis of densification behavior with the microstructural evolution during sintering.

The starting powder used in this study was a high-purity stoichiometric $MgAl_2O_4$ spinel powder (TSP-15, Taimei Chemical Co., Ltd., Tokyo, Japan) with a purity of >99.97%. The TEM observation confirmed that the powder consists of fine particles with a diameter range of 100–300 nm. For the as-received powder, defects, such as dislocations and stacking faults, are limited. The powder was sintered using an SPS machine (SPS-1050, SPS Syntex Inc., Kawasaki, Japan) and a graphite die having a 30 mm inner diameter. Under the conditions of vacuum and a uniaxial pressure of 80 MPa, the powder was heated to the desired temperatures at the heating rate of 10 °C min^{-1} at above 1000 °C. The temperature was controlled by monitoring the surface temperature T_s of the graphite die using an optical pyrometer.

In order to correct the temperature difference between the die outer surface and the powder, the true sintering temperature T_t of the powder was measured at $T_s = 1000$–1400 °C using an R-type thermocouple, which was inserted directly into the powder placed in the graphite die. The relation between T_s and T_t can be expressed by $T_t = 1.063T_s - 27$ in °C.

The microstructures were examined around the center of the SPSed disks by scanning electron microscopy (SEM) and transmission electron microscopy (TEM). In order to examine the microstructural evolution during the SPS processing, the sintering was interrupted at the desired densities. For the SEM observations, the microstructure was observed at the fracture surface. For the TEM observations, thin sheets with a thickness of about 500 μm were cut perpendicular to the compressive axis. The sheets were mechanically polished to a thickness of about 100 μm and followed by further thinning using an Ar ion-milling machine.

* Corresponding author. Tel.: +81 29 859 2537; fax: +81 29 859 2501; e-mail: MORITA.Koji@nims.go.jp

1359-6462/$ - see front matter © 2010 Acta Materialia Inc. Published by Elsevier Ltd. All rights reserved.
doi:10.1016/j.scriptamat.2010.06.012

The relative density ρ_t at the instantaneous processing time t was evaluated as $\rho_t = \rho_f\ (h_f/h_t)$, where ρ_f is the final relative density measured by Archimedes method using the theoretical density of $3.584 \times 10^3\ \mathrm{kg\ m^{-3}}$, h_f is the final sample height and h_t is the sample height at the instantaneous processing time t. h_t was calculated from the relative displacement of the moving ram of the SPS machine by correcting the thermal expansion of the system, which was measured separately by dummy tests using the same heating process.

Under the present SPS condition, the densification rate $\dot{\rho}_t$ $(=(1/\rho_t)(d\rho_t/dt))$ became a maximum at around $T_s = 1150$–$1200\ ^\circ\mathrm{C}$ [4]. In the present study, we examined the densification behavior of the spinel powder at $T_s = 1175\ ^\circ\mathrm{C}$; that is, $T_t = 1222\ ^\circ\mathrm{C}$. Figure 1 shows an example of ρ_t plotted as a function of the soaking time t_s. For the initial stage of the SPS processing of the spinel, Bernard-Granger et al. [6] reported a density plateau in the densification curve, where the density remained an almost constant value for a certain period. In the present study, however, the densification curves of the stoichiometric spinel show normally observed sintering behavior similar to that of hot-pressing [7], for which the densification rate continuously decreases with t_s.

The densification rate $\dot{\rho}_t$ during the pressure sintering process can be considered as analogous to high-temperature deformation and can be characterized by the following equation [6–9]:

$$\dot{\rho}_t = A d^{-p} \left(\frac{\sigma_{eff}}{G_{eff}}\right)^n \exp\left(-\frac{Q}{RT}\right) \tag{1}$$

where σ_{eff} and G_{eff} are the effective stress and the effective shear modulus at the instantaneous density ρ_t, respectively, n is the stress exponent, d is the grain size, p is the grain size exponent, Q is the apparent activation energy, R is the gas constant, T is the absolute temperature and A is a constant. σ_{eff} and G_{eff} of porous ceramics can be expressed as a function of ρ_t as follows [10,11]:

$$\sigma_{eff} = \frac{1-\rho_0}{\rho_t^2(\rho_t-\rho_0)}\sigma_{app} \quad (\text{for } \rho_t < 90\%) \tag{2}$$

and

$$G_{eff} = \frac{E_{th}}{2(1+\nu_{eff})}\frac{\rho_t-\rho_0}{1-\rho_0} \tag{3}$$

where ρ_0 is the initial relative density, σ_{app} is the applied stress, E_{th} is the theoretical Young's modulus of a dense material ($E_{th} = 233$ GPa at $T_t = 1222\ ^\circ\mathrm{C}$ [12]) and ν_{eff} is the effective Poisson's ratio and can be regarded the same as that of dense materials (0.25 [13]). In this study, the ρ_0-value was measured at $T_s = 1000\ ^\circ\mathrm{C}$, at which the apparent densification starts, and was estimated to be about 58%.

Figure 2 shows the $\dot{\rho}_t$–(σ_{eff}/G_{eff}) relationship evaluated from the densification curve shown in Figure 1. As σ_{eff} decreases, that is, as ρ_t increases, $\dot{\rho}_t$ decreases steeply around $\rho_t = 74$–77% and gradually at $\rho_t \leqslant 80\%$. The densification mechanism has generally been characterized by the stress exponent n defined by Eq. (1). Although the n-value should be determined for the same grain size, the grain growth takes place from $d = 130$ nm to $d = 500$ nm during the sintering, as shown in Figure 1. Accordingly, the correction of the grain size is necessary to estimate the true n-value, particularly for the low σ_{eff} (high ρ_t) region. The correction using $p = 2$ [7] shifts the $\dot{\rho}_t$–σ_{eff} relationship slightly to the high $\dot{\rho}_t$ region but does not change the general feature, as indicated by the triangles. The stress exponent evaluated from the corrected $\dot{\rho}_t$–σ_{eff} relationship can be characterized by $n \geqslant 4$ in the low ρ_t region and by $n \approx 1$ in the high ρ_t region, and the two regions may be connected by $n \approx 2$ at intermediate ρ_t. The corrected $\dot{\rho}_t$–σ_{eff} relationship reveals a trend similar to those of the hot-pressed spinels [7,14–16].

The substructure during SPS processing was examined at several ρ_t values in Figure 3. In order to prevent the annealing-out of substructures developed during the SPS processing, the specimens were sintered up to the desired densities and cooled under loading. Although a high-resolution TEM observation was performed at several densities of $\rho_t = 74$–98%, the present material was monolithic and no amorphous phases were found along the boundaries and at multiple-grain junctions. An

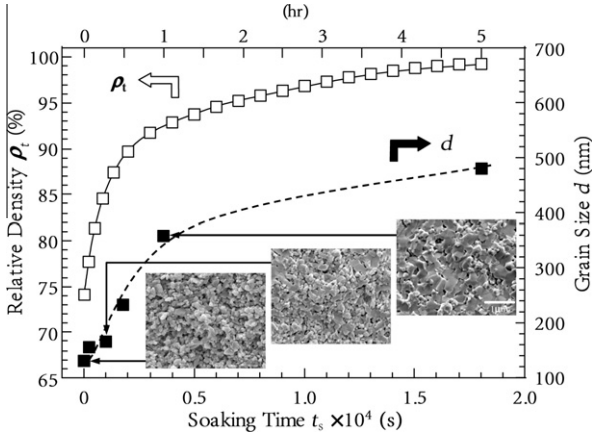

Figure 1. Densification curves (□) and grain size (■) tested at $T_t = 1222\ ^\circ\mathrm{C}$ plotted as a function of the soaking time t_s. SEM images show the typical microstructure SPSed up to the respective densities of $\rho_t = 74$, 86 and 93%.

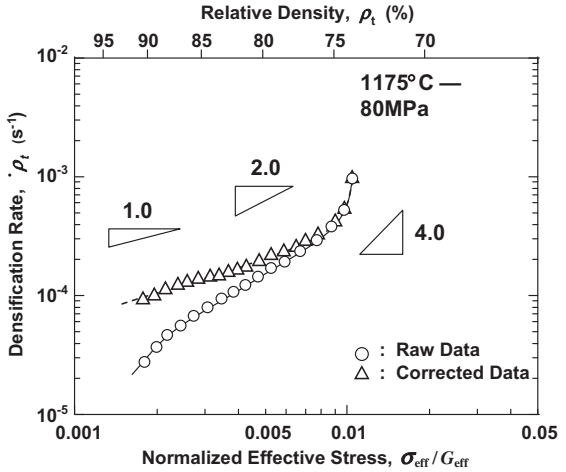

Figure 2. Densification rate $\dot{\rho}_t$ $(=(1/\rho_t)(d\rho_t/dt))$ plotted as a function of the normalized effective stress (σ_{eff}/G_{eff}).